Available online at www.sciencedirect.com

SciVerse ScienceDirect

Ceramics International 39 (2013) 5925–5930

CERAMICS INTERNATIONAL

www.elsevier.com/locate/ceramint

# Structural and electrical properties of NBT–$BT_{0.08}$ ceramic prepared by the pyrosol method

Cristina Ghitulica[a], Marin Cernea[b], Bogdan Stefan Vasile[a,*], Ecaterina Andronescu[a], Otilia Ruxandra Vasile[a], Cristina Dragoi[b], Roxana Trusca[c]

[a]*University Politehnica of Bucharest, Faculty of Applied Chemistry and Material Science, Department of Science and Engineering of Oxide Materials and Nanomaterials, No. 1-7 Gh. Polizu Street, 011061 Bucharest, Romania*

[b]*National Institute of Materials Physics, P.O. Box MG-7, Bucharest-Magurele, 077125, Romania*

[c]*METAV-R&D S. A., P.O. 22, Bucharest, Romania*

Received 23 November 2012; received in revised form 18 December 2012; accepted 7 January 2013
Available online 16 January 2013

**Abstract**

$[(Bi_{0.5}Na_{0.5})TiO_3]_{0.92}$–$[BaTiO_3]_{0.08}$ lead free piezoelectric materials were prepared by the pyrosol method. The as-obtained powder shows spherical grains of various sizes, composed of crystallites of about 10 nm. NBT–$BT_{0.08}$ ceramic obtained at 700 °C show rhombohedral NBT as the main phase and traces of hexagonal $Bi_2O_3$ as secondary phase. The ceramics prepared from this powder and sintered at 1000 and 1100 °C are single phase with good dielectric and ferroelectric properties.


*Keywords:* A. Pyrosol processes; C. Dielectric properties; C. Piezoelectric properties; D. $BaTiO_3$ and titanates

## 1. Introduction

The lead-free piezoelectric ceramics present a great interest as potential substitutes for lead piezoelectric ceramics. Lead-free piezoelectric materials include $BaTiO_3$, (Na,Bi)$TiO_3$, (Na,K)$NbO_3$ system and so on [1]. $Na_{1/2}Bi_{1/2}TiO_3$ (NBT) is a ferroelectric compound, with perovskite structure, which exhibits weak piezoelectric properties [2,3]. A large number of NBT-based solid solutions, including NBT–$BaTiO_3$ (NBT–BT), have been prepared and intensively studied in the recent years [4–15]. The $(1-x)$NBT–$x$BT (abbreviated as NBT–$BT_x$) ceramics, with 1–20 mol% $BaTiO_3$, show improved piezoelectric properties, lower Curie temperature and higher sintering ability, compared with the NBT ceramic. NBT–$BT_x$ ceramics have been prepared by various methods, such as conventional solid state reaction [16,17], citrate method [18,19], emulsion method [20], hydrothermal process [21], sol–gel techniques [22,23] and stearic acid sol–gel route [24]. Recently, the pyrosol method has been used to produce fine powders [25–29]. By pyrosol method, powders with grains of various diameters were obtained, non-agglomerated, that is an advantage for densification of the compacted powders by pressing. It is well-known that the pressing of the powder is enhanced when the grains have different sizes. Therefore, the shape and size of the grains are important factors that influence the macroscopic properties of the ceramics.

To our knowledge, there are no reports about the synthesis by pyrosol of NBT–$BT_{0.08}$. In the present study, NBT–$BT_{0.08}$ ceramics were prepared by the pyrosol method, and their structure and electrical properties were examined. We chosen $x=0.08$ for BNT–bt$x$ in order to have a composition near MPB region (BNT–bt$x$, $x=0.06$–0.07) were BNT–bt$x$ ceramics show good dielectric, ferroelectric, piezoelectric, and pyroelectric properties, and a relatively easy electric poling.

## 2. Experimental procedure

$[(Bi_{0.5}Na_{0.5})TiO_3]_{0.92}$–$[BaTiO_3]_{0.08}$ was prepared by a pyrosol technique starting from anhydrous sodium acetate

*Corresponding author. Tel./fax: +4021 310 76 33.
*E-mail address:* bogdan.vasile@upb.ro (B. Stefan Vasile).

0272-8842/$ - see front matter © 2013 Elsevier Ltd and Techna Group S.r.l. All rights reserved.
http://dx.doi.org/10.1016/j.ceramint.2013.01.015

($CH_3COONa$, 99.995%, Aldrich), barium acetate (($CH_3COO)_2Ba$, 99%, Aldrich), bismuth (III) acetate (($CH_3COO)_3Bi$, +99.99%, Aldrich) and titanium (IV) isopropoxide, 97% solution in 2-propanol ($Ti\{OCH(CH_3)_2\}_4$, Aldrich). Acetic acid (≥99.7%, Aldrich) was used as a solvent for the acetate salts. Sodium acetate, bismuth (III) acetate and barium acetate were dissolved separately in water and acetic acid at about 100 °C. Titanium (IV) isopropoxide was then added gradually to the mixture of these solutions. A clear solution was obtained by adding nitric acid. The concentration of the sol was brought to the value 0.4 M with strong magnetic agitation at 75 °C for 6 h. An aerosol has been formed from the solution of precursors using a high-frequency ultra sound generator. The aerosol is carried through a tubular furnace heated at 700 °C, in a quartz tube, by a carrier nitrogen gas. At the end of the tube, a high-voltage Mo wire collects the ceramic powder [25,26]. The ceramic samples were prepared by uniaxially pressing of powders into discs (1.2 cm diameter and ~0.2 cm thick), using a pressure of 100 MPa and then sintered at temperatures of 1000 °C and 1100 °C, for 2 h in air.

The phase composition and microstructure of NBT–$BT_{0.08}$ powder and ceramic were investigated by X-ray diffraction (XRD), scanning electronic microscopy (SEM) and transmission electronic microscopy (TEM). The composition of the NBT–$BT_{0.08}$ precursor powders was characterized by X-ray diffraction technique using a Bruker-AXS tip D8 ADVANCE diffractometer. For powder diffraction, Cu$K_{\alpha 1}$ radiation (wavelength 1.5406 Å), LiF crystal monochromator and Bragg–Brentano diffraction geometry were used. The data were acquired at 25 °C with a step-scan interval of 0.020° and a step time of 10 s. The microstructure of the samples was investigated using a FEI Quanta Inspect F with EDAX scanning electron microscope and, a Tecnai™ $G^2$ F30 S-TWIN transmission electron microscope with a line resolution of 1 Å, in high resolution transmission electron microscopy (HR-TEM) mode and selected area electron diffraction (SAED). The electrical measurements of NBT–$BT_{0.08}$ ceramic pellets were carried out in the metal–ferroelectric-metal (MFM) configuration, where the electrodes M consist of silver paste. Dielectric measurements at frequency range of 10 kHz–1 MHz have been performed at room temperature, using a Hioki 3532-50 type automatic RLC bridge. *P–E* loops were measured using a TF Analyzer 2000 equipped with a FE-Module (aixACCT).

## 3. Results and discussion

### 3.1. X-ray diffraction

X-ray diffraction patterns of the of NBT–$BT_{0.08}$ powder, prepared by pyrosol technique at 700 °C and annealed at 700–900 °C, are shown in Fig. 1.

The XRD analyses indicate the presence of two phases. The diffraction peaks of the main phase can be assigned to the rhombohedral polymorphic modification of NBT (Fig. 1(a)) (Pattern: 01-070-9850) [30]. The peaks of the secondary phase can be attributed to the $Bi_2O_3$ hexagonal phase (Pattern: 51-1161) [31]. The feature peak at about 47° does not split in the figure, which indicates that all ceramics have rhombohedral microstructure.

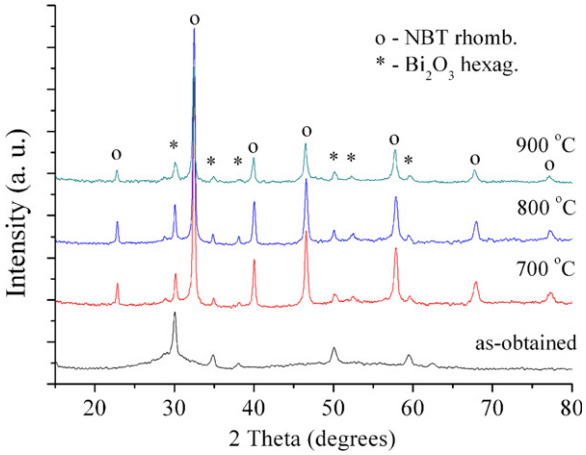


Fig. 1. XRD patterns of NBT–$BT_{0.08}$ powder obtained by pyrosol method at 700 °C (a) and then calcined at 700 °C (3 h), 800 °C (2 h) and 900 °C, 2 h.

### 3.2. SEM analysis

The SEM micrographs of $Na_{0.5}Bi_{0.5}TiO_3$ doped with 8 mol% $BaTiO_3$, prepared by pyrosol method at 700 °C, and annealed at 700 °C, 3 h, in air, are presented in Fig. 2.

The majority of grains, for the powders resulted at 700 °C, show spherical shape but some grains have an irregular sphere or ring shape, due to the collision of sol droplets. The grains have diameter in the range 0.17–1 μm (Fig. 2(a)). The surface of NBT–$BT_{0.08}$ powder grains presents roughness, due to the pyrolysis of organic part from the precursor. After heating the powders at 700 °C, 3 h in air, the grains acquire a cubic form with an average size of 400 nm (Fig. 2(b)).

### 3.3. TEM–HRTEM–SAED analyses

The NBT–$BT_{0.08}$ as-obtained powders by pyrosol (Fig. 3) and then annealed at 700 °C, for 3 h in air (Fig. 4) were investigated by TEM, with the aim of studying the evolution of crystallites with the annealing time.

TEM image of the powder shows spherical grains (Fig. 3(a)) of various sizes, composed from crystallites Fig. 3(b) of about 10 nm. The incomplete crystallization of the powder of NBT–$BT_{0.08}$ is evidenced by the HR-TEM image and the SAED pattern (Fig. 3(c)). The Fig. 3 (b) shows a lattice fringe of $d$=2.24 Å, corresponding to the (202) crystallographic plane of rhombohedral $Ba_{0.5}Na_{0.5}TiO_3$. Other crystallographic planes, identified on the SAED pattern, are (404) and (300), indicated that the

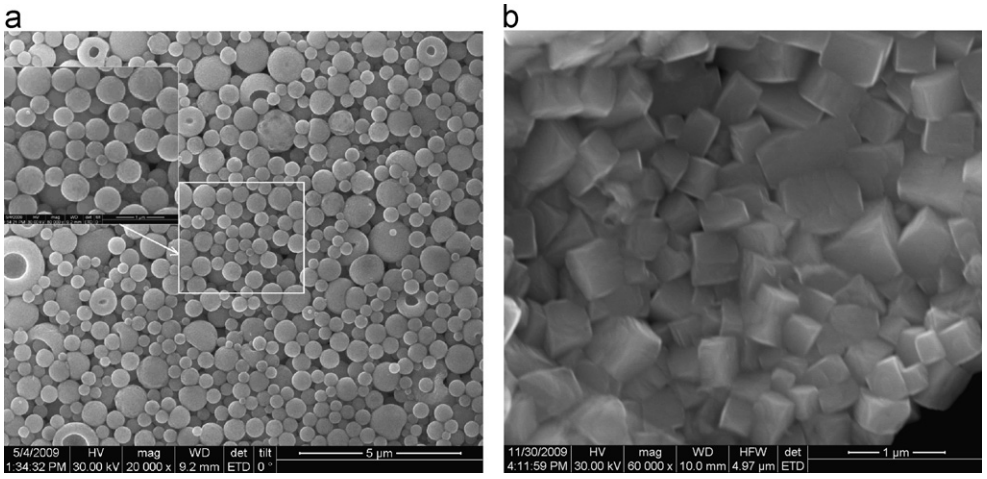


Fig. 2. SEM photomicrographs of NBT–$BT_{0.08}$ powder obtained by pyrosol method at 700 °C (a), annealed at 700 °C, 3 h in air (b).

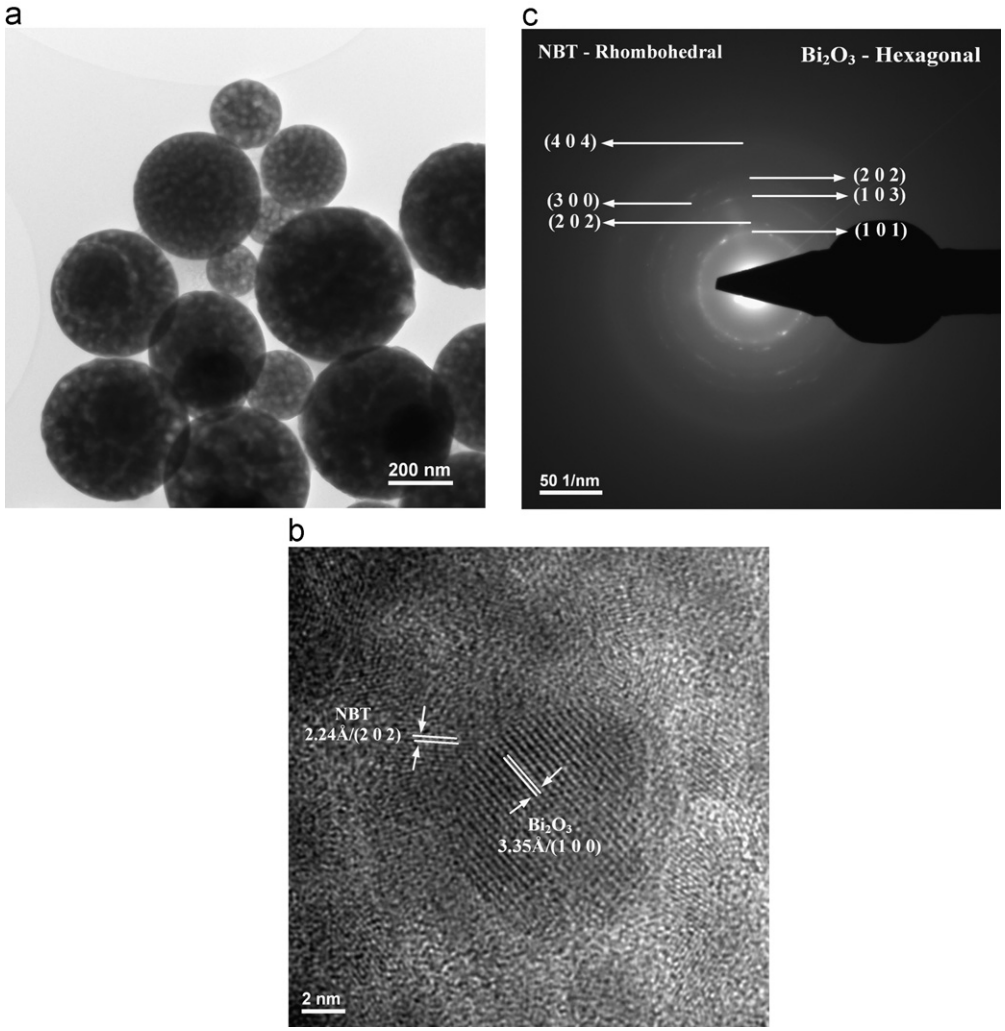


Fig. 3. TEM (a), HR-TEM (b) and SAED (c) images of NBT–$BT_{0.08}$ powder prepared by pyrosol at 700 °C.

crystallization of the rhombohedral NBT phase start even in the powder as-obtained by the pyrosol method. The rhombohedral NBT phase is not indicated by X-ray diffraction (Fig. 1). The HR-TEM image and SAED pattern confirm that the hexagonal $Bi_2O_3$ phase is the main phase in the powder as-obtained by pyrosol at 700 °C

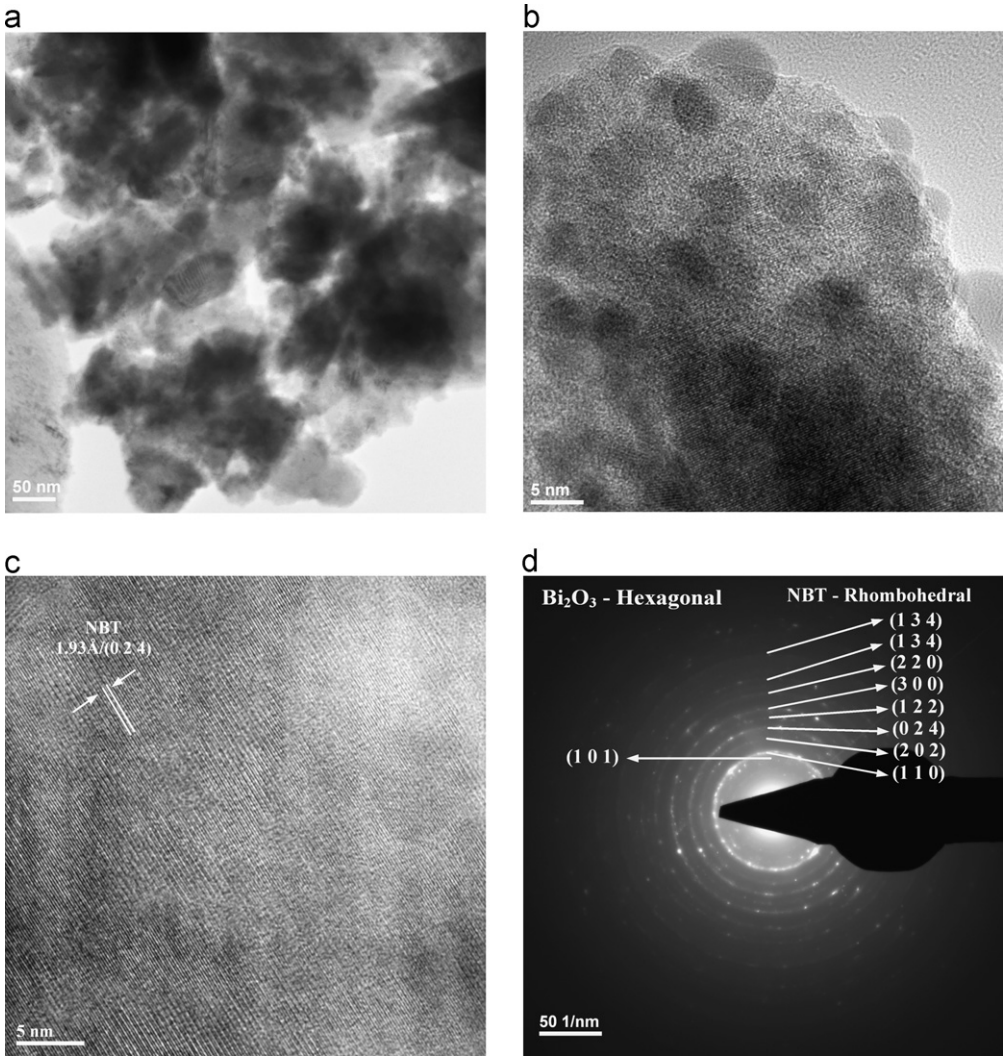


Fig. 4. TEM (a, b), HR-TEM (c) and SAED (d) images of NBT–$BT_{0.08}$ powder prepared by pyrosol at 700 °C and annealed at 700 °C, for 3 h in air.

(lattice fringe corresponding to the crystallographic planes (202), (103), (101) and, (100)/$d$=3.35 Å).

TEM investigations on the NBT–$BT_{0.08}$ powder prepared by pyrosol at 700 °C and annealed at 700 °C, for 3 h, in air, show grains with polyhedral shape and crystallites well crystallized of about 20 nm size (Fig. 4).

Fig. 4(c),(d) shows lattice fringe of $d$=1.93 Å corresponding to the (024) crystallographic plane and, others planes (110), (202), (122) of rhombohedral $Ba_{0.5}Na_{0.5}TiO_3$ (Fig. 4(c)).

### 3.4. Sintering behavior and piezoelectric characterization

NBT–$BT_{0.08}$ ceramic were characterized in what concers their aparet density, the values obtained are in the range of 92–94% of the theoretical density were measured by Archimedes's method (in water) using a density balance. Fig. 5 shows the SEM micrographs of the NBT–$BT_{0.08}$ samples sintered at 1000 °C and 1100 °C. The pellets show grains with polyhedral shape and average grains size of 0.9 μm and 2 μm, respectively, as it can be seen in Fig. 5.

Fig. 6 shows the XRD patterns of the NBT–$BT_{0.08}$ ceramic sintered at 1000 °C and 1100 °C. X-ray patterns of NBT–$BT_{0.08}$ ceramics sintered at 1000 °C, for 2 h in air, exhibit peaks corresponding to the rhombohedral NBT structure [30] (Fig. 6(a)). The NBT–$BT_{0.08}$ ceramic sintered at 1100 °C shows peaks of the rhombohedral NBT structure (Fig. 6(b)), but the ratio of their intensities is different from those of XRD patterns of the NBT–$BT_{0.08}$ ceramic sintered at 1000 °C. That suggest the starting the process of degradation of the structure of NBT–$BT_{0.08}$ ceramic, by evaporation of bismuth, at 1100 °C. By comparison with the NBT–$BT_{0.08}$ powder, the ceramic is not showing any secondary phase.

### 3.5. Dielectric characterization

The permittivity frequency and the dissipation factor frequency curves for the NBT–$BT_{0.08}$ ceramic sintered at 1000 °C, 2 h, in air, are shown in Fig. 7. It can be observed

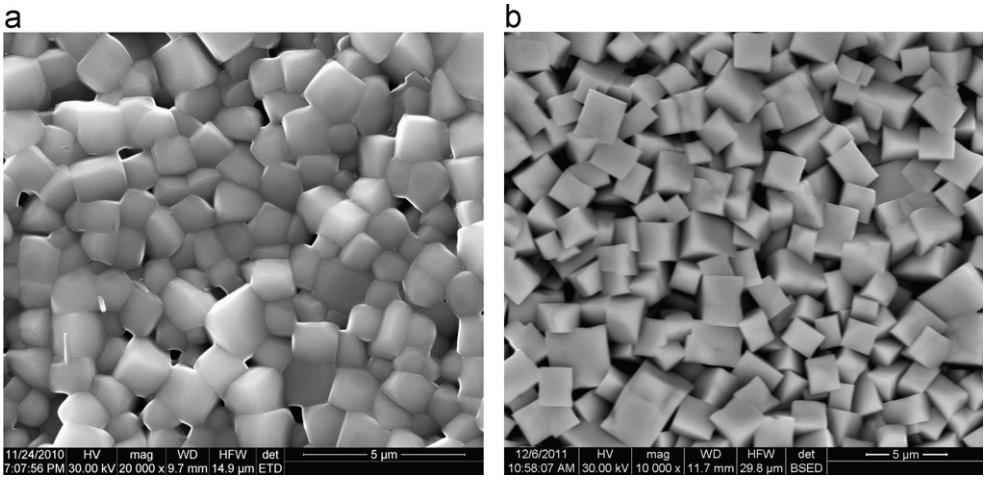


Fig. 5. SEM images of NBT–$BT_{0.08}$ ceramic sintered at 1000 °C (a) and 1100 °C (b).

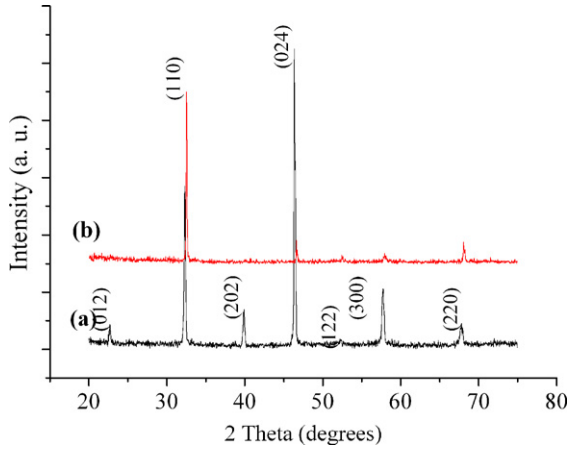


Fig. 6. XRD patterns of NBT–$BT_{0.08}$ pellets sintered at 1000 °C (a) and 1100 °C (b), for 2 h in air.

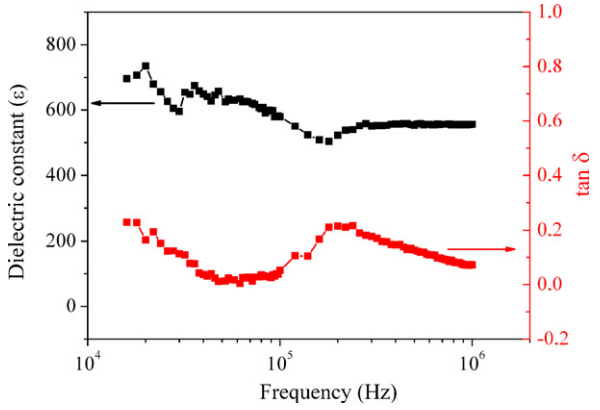


Fig. 7. Frequency dependence of dielectric constant and dielectric loss of NBT–$BT_{0.08}$ ceramic sintered at 1000 °C.

that the dielectric constants and loss tangent of NBT–$BT_{0.08}$ ceramic decrease with the increase of the frequency.

As it can be seen in Fig. 7, neither the dielectric constant, nor the dielectric losses, are significantly influenced by

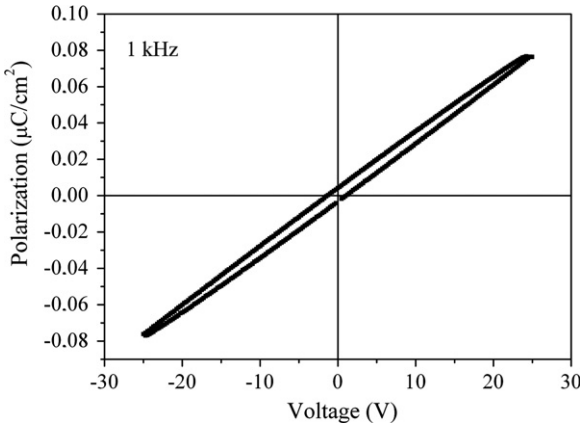


Fig. 8. Room temperature ferroelectric hysteresis loops measured for the NBT–$BT_{0.08}$, for an applied voltage ranging from −30 to 30 V.

frequency (in the $10^4$–$10^6$ Hz domain), suggesting a good homogeneity of samples. The dielectric constant ($\varepsilon_r = 600$) and the dielectric loss ($\tan\delta = 0.05$), measured at 100 kHz, of the NBT–$BT_{0.08}$ ceramic samples, were comparable with that prepared by sol–gel process [23].

Fig. 8 shows the P– E hysteresis loop of the NBT–$BT_{0.08}$ at 1 kHz at room temperature. The P–E hysteresis loop shows a narrow type, without saturation in polarization. Such a phenomenon is considered to be based on a random field resulting from fine-scale domains, due to defects at A-sites of perovskite compounds, preventing a complete polarization switching [32]. The dielectric and ferroelectric properties of NBT–$BT_{0.08}$ ceramic were comparable with those of NBT–$BT_{0.08}$ derived from sol–gel processes.

## 4. Conclusions

In the current work, a wet-chemistry synthesis route, pyrosol, was chosen to synthesize high purity NBT–$BT_{0.08}$ powders. The powder obtained at 700 °C shows spherical grains of various sizes, composed from crystallites of about 10 nm. The powders show $Bi_2O_3$ as secondary phase but

the ceramic sintered at temperatures higher than 1000 °C was obtained as single phase. The dielectric and ferroelectric characteristic of NBT–$BT_{0.08}$ ceramic processed by pyrosol are suitable for applications in microelectronics.

## Aknowledgements

The authors gratefully acknowledge the Romanian Research Ministry PNCDI II, Contract no. 72-153/2008, and the Sectorial Operational Programme Human Resources Development, financed from the European Social Fund and by the Romanian Government under the contract number POSDRU/107/1.5/S/76813 for financial support.

## References

[1] D.Q. Zhang, Z.C. Qin, X.Y. Yang, H.B. Zhu, M.S. Cao, Study on synthesis and evolution of sodium potassium niobate ceramic powders by an oxalic acid-based sol–gel method, Journal of Sol–Gel Science and Technology 57 (2011) 31–35.

[2] C. Xu, D. Lin, K.W. Kwok, Structure, electrical properties and depolarization temperature of $(Bi_{0.5}Na_{0.5})TiO_3$–$BaTiO_3$ lead-free piezoelectric ceramics, Solid State Sciences 10 (2008) 934–940.

[3] A. Herabut, A. Safari, Processing and electromechanical properties of $(Bi_{0.5}Na_{0.5})(1-1.5_x)La_xTiO_3$ ceramics, Journal of the American Ceramic Society 80 (1997) 2954–2958.

[4] K. Yoshii, Y. Hiruma, H. Nagata, T. Takenaka, Electrical properties and depolarization temperature of $(Bi_{1/2}Na_{1/2})TiO_3$–$(Bi_{1/2}K_{1/2})TiO_3$ Lead-free Piezoelectric Ceramics, Japanese Journal of Applied Physics 45 (2006) 4493–4496.

[5] S. Zhao, G. Li, A. Ding, T. Wang, Q. Rui, Ferroelectric and piezoelectric properties of $(Na, K)_{0.5}Bi_{0.5}TiO_3$ lead free ceramics, Journal of Physics D: Applied Physics 39 (2006) 2277.

[6] Y.M. Li, W. Chen, J. Zhou, Q. Xu, H.J. Sun, R.X. Xu, Dielectric and piezoelecrtic properties of lead-free $(Na_{0.5}Bi_{0.5})TiO_3$–$NaNbO_3$ ceramics, Materials Science and Engineering B 1122 (2004) 5–9.

[7] X.X. Wang, X.G. Tang, K. Kwok, H.L.W. Chan, C.L. Choy, Effect of excess $Bi_2O_3$ on the electrical properties and microstructure of $(Bi_{1/2}Na_{1/2})TiO_3$ ceramics, Applied Physics A 80 (2005) 1071–1075.

[8] D. Lin, D. Xiao, J. Zhu, P. Yu, Piezoelectric and ferroelectric properties of $[Bi_{0.5}(Na_{1-x-y}K_xLi_y)_{0.5}]TiO_3$ lead-free piezoelectric ceramics, Applied Physics Letters 88 (2006) 062901.

[9] D. Lin, D. Xiao, J. Zhu, P. Yu, Piezoelectric and ferroelectric properties of lead-free $[Bi_{1-y}(Na_{1-x-y}Li_x)]_{0.5}Ba_yTiO_3$ ceramics, Journal of the European Ceramic Society 26 (2006) 3247–3251.

[10] Y.M. Li, W. Chen, Q. Xu, J. Zhou, X. Gu, S. Fang, Electromechanical and dielectric properties of $Na_{0.5}Bi_{0.5}TiO_3$–$K_{0.5}Bi_{0.5}TiO_3$–$BaTiO_3$ lead-free ceramics, Materials Chemistry and Physics 94 (2005) 328–332.

[11] J. Shieh, K.C. Wu, C.S. Chen, Switching characteristics of MPB compositions of $(Bi_{0.5}Na_{0.5})TiO_3$–$BaTiO_3$–$(Bi_{0.5}K_{0.5})TiO_3$ lead-free ferroelectric ceramics, Acta Materialia 55 (2007) 3081–3087.

[12] S. Zhang, T.R. Shrout, H. Nagata, Y. Hiruma, T. Takenaka, Piezoelectric properties in $(K_{0.5}Bi_{0.5})TiO_3$–$(Na_{0.5}Bi_{0.5})TiO_3$–$BaTiO_3$ lead-free ceramics, IEEE Transactions on Ultrasonics, Ferroelectrics, and Frequency Control 54 (2007) 910–917.

[13] B.J. Chu, D.R. Chen, G.R. Li, Q.R. Yin, Electrical properties of $Na_{1/2}Bi_{1/2}TiO_3$–$BaTiO_3$ ceramics, Journal of the European Ceramic Society 22 (2002) 2115–2121.

[14] R. Ranjan, A. Dviwedi, Structure and dielectric properties of $(Na_{0.50}Bi_{0.50})_{1-x}Ba_xTiO_3$: $0 \le x \le 0.10$, Solid State Communications 135 (2005) 394–399.

[15] X.Y. Zhou, H.S. Gu, Y. Wang, W.Y. Li, T.S. Zhou, Piezoelectric properties of Mn-doped $(Na_{0.5}Bi_{0.5})_{0.92}Ba_{0.08}TiO_3$ ceramics, Materials Letters 59 (2005) 1649–1652.

[16] Y.F. Wei, H.H. Chung, C.F. Yang, K.H. Chen, C.C. Diao, C.H. Kao, The influence of different fabrication processes on characteristics of excess $Bi_2O_3$-doped $0.95(Na_{0.5}Bi_{0.5})TiO_{3-0.05}$ $BaTiO_3$ceramics, Journal of Physics and Chemistry of Solids 69 (2008) 934–940.

[17] W.C. Lee, C.Y. Huang, L.K. Tsao, Y.C. Wu, Chemical composition and tolerance factor at the morphotropic phase boundary in $(Bi_{0.5}Na_{0.5})TiO_3$-based piezoelectric ceramics, Journal of the European Ceramic Society 29 (2009) 1443–1448.

[18] D.L. West, D.A. Payne, Preparation of $0.95Bi_{1/2}Na_{1/2}TiO_3 \cdot 0.05BaTiO_3$ Ceramics by an Aqueous Citrate–Gel Route, Journal of the American Ceramic Society 86 (2003) 192–194.

[19] M. Chen, Q. Xu, B.H. Kim, B.K. Ahn, J.H. Ko, W.J. Kang, O.J. Nam, Structure and electrical properties of $(Na_{0.5}Bi_{0.5})_{1-x}Ba_xTiO_3$piezoelectric ceramics, Journal of the European Ceramic Society 28 (2008) 843–849.

[20] B.H. Kim, S.J. Han, J.H. Kim, J.H. Lee, B.K. Ahn, Q. Xu, Electrical properties of $(1-x)(Bi_{0.5}Na_{0.5})TiO_3$–$xBaTiO_3$synthesized by emulsion method, Ceramics International 33 (2007) 447–452.

[21] P. Pookmanee, G. Rujijanagul, S. Ananta, R.B. Heimann, S. Phanichphant, Effect of sintering temperature on microstructure of hydrothermally prepared bismuth sodium titanate ceramics, Journal of the European Ceramic Society 24 (2004) 517–520.

[22] E. Mercadelli, C. Galassi, A.L. Costa, S. Albonetti, A. Sanson, Sol–gel combustion synthesis of BNBT powders, Journal of Sol–Gel Science and Technology 46 (2008) 39–45.

[23] M. Cernea, B.S. Vasile., C. Capiani, A. Ioncea, C. Galassi, Dielectric and piezoelectric behaviors of NBT–$BT_{0.05}$ processed by sol–gel method, Journal of the European Ceramic Society 32 (2012) 133–139.

[24] J. Hao, X.H. Wang, R.Z. Chen, L.T. Li, Synthesis of $(Bi_{0.5}Na_{0.5})$-$TiO_3$ nanocrystalline powders by stearic acid gel method, Materials Chemistry and Physics 90 (2005) 282–285.

[25] E. Dinu, E. Andronescu, C.D. Ghitulica, E. Siebert, E. Djurado, L. Dessemond, Nanocrystallites obtained through the pyrosol method, Physica Status Solidi A 205 (2008) 1488–1493.

[26] B.S. Vasile, O.R. Vasile, C. Ghitulica, E. Andronescu, R. Dobranis, E. Dinu, R. Trusca, Yttria totally stabilized zirconia nanoparticles obtained through the pyrosol method, Physica Status Solidi A 207 (2010) 2499–2504.

[27] B. Gharbage, M. Henault, T. Pagnier, A. Hammou, Preparation of $La1-xSrxMnO_3$ thin films by a pyrosol derived method, Materials Research Bulletin 26 (1991) 1001–1007.

[28] C. Lee, K. Lim, J. Song, Highly textured ZnO thin films doped with indium prepared by the pyrosol method, Solar Energy Materials and Solar Cells 43 (1996) 37–45.

[29] M.N. Islam, M.O. Hakim, A simple technique for the pyrosol process and deposition of tin oxide films, Journal of Physics and Chemistry of Solids 46 (1985) 339–343.

[30] G.O. Jones, P.A. Thomas, Investigation of the structure and phase transitions in the novel A-site substituted distorted perovskite compound $Na_{0.5}Bi_{0.5}TiO_3$, Acta Crystallographica Section B: Structural Science 58 (2002) 168–178 Pattern: 01-070-9850.

[31] T. Atou, H. Faqir, M. Kikuchi, H. Chiba, Y. Syono, Structure Determination of Ferromagnetic Perovskite $BiMnO_3$, Journal of Solid State Chemistry 145 (1999) 639–642.

[32] M. Md., N. Rahman, Yasuda, Electric field-induced switching of nanometer-sized twin related domains in $0.91Pb(Zn_{1/3}Nb_{2/3})O_3$–$0.09PbTiO_3$ single crystal near a morphotropic phase boundary composition, Solid State Communications 149 (2009) 630–633.